Physical Characterization and Comparison of Doppler and Attitude Estimates for ENVISAT/ASAR and RADARSAT-1

Marina V. Dragošević, Riccardo Ferrara
Advanced Computer Systems S.p.A.

Via della Bufalotta 378, 00139 Rome, Italy
Emails: m.dragosevic@acsys.it, r.ferrara@acsys.it

INTRODUCTION

ENVISAT and RADARSAT-1 both carry multi-beam SAR sensors operating in C-band at similar radar frequencies from similar orbits. There are also important differences between the two systems: the ASAR steering strategy, its active antenna array, the choice of polarizations and different burst strategies. The common features and the differences make the Doppler estimation issue an interesting topic for a comparative analysis.

ACS has developed an adaptive and efficient generic SAR processor, GASP, which includes several algorithms related to Doppler and attitude estimation and tracking. They are used routinely during image formation. This has allowed us to compare the performance of the same estimation methods for different SAR data sources.

An intrinsic feature of the implemented estimation methods is the Doppler centroid model and parameterization in terms of the physical properties of the sensor, the attitude of the platform and the state of relative motion. In order to make such an approach meaningful, it is important to characterize the system precisely enough, using pre-launch measurements, current instrument characterization data, as well as in-flight monitoring and analysis of the telemetry. Certain systematic offsets, misalignments or nonlinearities can be identified from an accumulation and off-line analysis of Doppler and attitude estimates [9]. We have observed and we have tried to quantify some of them. Then we have included them in the processor via configurable system characterization input files, customized for each mission.

BASIC DOPPLER CENTROID MODELS

The Doppler centroid (DC) f_c, as a function of the elevation angle γ can be expressed in terms of the directly or indirectly available measurements in one of the following ways:

$$f_c(\gamma) = \underbrace{f_t(\gamma) + f_m(\gamma)}_{\text{reference}} + (\hat{\phi}_y \sin\gamma - \hat{\phi}_p \cos\gamma) f_a + \epsilon(\gamma) \quad (1)$$

$$f_c(\gamma) = \frac{f_0}{f_\Delta} \underbrace{\left(\hat{f}_H(\gamma) - \hat{f}_L(\gamma)\right)}_{\text{from sub-bands}} + E(\gamma) \quad (2)$$

$$f_c(\gamma) = \underbrace{\hat{n} f_p}_{\text{ambiguity}} + \hat{f}(\gamma) + e(\gamma) \quad (3)$$

All of the above forms are well known. The specific terms are defined in the Appendix.

First, DC is expressed in terms of the measured or estimated attitude variations (yaw $\hat{\phi}_y$ and pitch $\hat{\phi}_p$) from some reference values, corresponding to the reference (expected) DC. This reference DC includes the deterministic term $f_t(\gamma)$ (due to the transversal component of the relative velocity) and the term $f_m(\gamma)$

which captures the specific behavior of the particular system (modeled as beam mispointing, steering, offsets, misalignment). We refer to this form as the **physical model**.

Next, DC is expressed in terms of the ambiguous DC estimates obtained from two range looks (high and low bands, separated by f_Δ, around the radar frequency f_0) at different ranges across the swath. This form is known as the **wavelength diversity model**, closely related to the class of PRF ambiguity resolvers based on λ diversity.

Finally, DC is expressed in terms of the ambiguity number n and ambiguous DC estimates, where we may use the look DC estimates $f\hat{(}\gamma) = (\hat{f}_H(\gamma) + \hat{f}_L(\gamma))/2$. Due to the explicit dependence on the pulse repetition frequency (PRF) f_p, this form is referred to as the **PRF ambiguity model** and it is associated with the ambiguity resolvers based on the PRF diversity in the multi-beam case. Such resolvers exploit the beam overlap strips within the swath, minimizing the norm of the error $\hat{n}^{(k+1)} f_p^{(k+1)} - \hat{n}^{(k)} f_p^{(k)} + \hat{f}^{(k+1)}(\gamma) - \hat{f}^{(k)}(\gamma)$ in the overlap between the k-th and $(k+1)$-th beam.

The error terms (ϵ, E and e) are due to the estimation errors, but they also include all unmodeled (unknown or random) physical properties of the sensor.

Each of the above models may be insufficient by itself. A combination of all three improves the accuracy and robustness of the DC estimate. The Doppler estimation problem is posed as a parameter estimation problem. DC is modeled as a smooth function of γ, parametrized by ϕ_y and ϕ_p. The problem is to estimate them using SAR echo data at various levels of processing in such a way that the estimates are consistent with all three DC models. In particular, the estimates must be consistent with the *a priori* knowledge of the attitude, should satisfy the λ diversity property, the "fractional" part of $f_c(\gamma)$ must be consistent with the ambiguous estimates across swath and, in the case of multiple beams, it should be consistent with the concatenation (PRF diversity) property.

The *a priori* model and the weights placed on these different requirements should be adjusted for a particular mission to reflect the level of knowledge and the precision of the physical characterization of that mission.

EFFICIENT DC ESTIMATION SCHEMES

DC estimation can be done concurrently with image formation in an efficient way. The combined processing scheme presumes block-wise data processing and block to block DC adaptation. The methodology applied in GASP consists of:

- Doppler feature extraction in signal and image domain;
- parameter estimation and refinement using the physical DC model.

The following features extracted from the signal or image data are used:

azimuth correlation coefficient of azimuth uncompressed or azimuth compressed complex data (SLC, IMS); the phase of the first correlation coefficient approximates the Doppler spectrum peak position [1] [3];

energy of the azimuth spectral looks of compressed multi-look data (SGF, IMP); it is matched against a set of conditional expectations of the look energy levels, each one calculated for a different hypothesized DC error;

residual scalloping level of azimuth compressed burst data (SN, SW, IMM, APM, WSM ...); it is then equalized by the slope of the azimuth antenna gain, which is shifted adaptively in order to minimize scalloping [4] [8].

Features extracted before azimuth compression lead to coarse and ambiguous DC estimates. Features extracted in image domain lead to DC refinement. The choice of the most efficient refinement algorithm clearly depends on the requested product type. The obtained coarse or refined DC estimates are range dependent. Their usefulness in the combined estimation scheme is subject to accurate characterization of the azimuth antenna beam pattern in terms of: peak position, integral corresponding to different looks or slope.

Parameter estimation means, in fact, fitting the attitude angles [5] [6] and, inherently, the ambiguity numbers, for all beams or polarizations simultaneously to the extracted features. It is carried out block by block using the coarsely estimated Doppler spectrum peak position in the latest data block, as well as the tracker state, which results from the DC refinement on previous blocks [7]. Attitude parameter tracking is related to the physical model (1), where the term $f_m(\gamma)$ has a particular form for RADARSAT-1 and for ASAR.

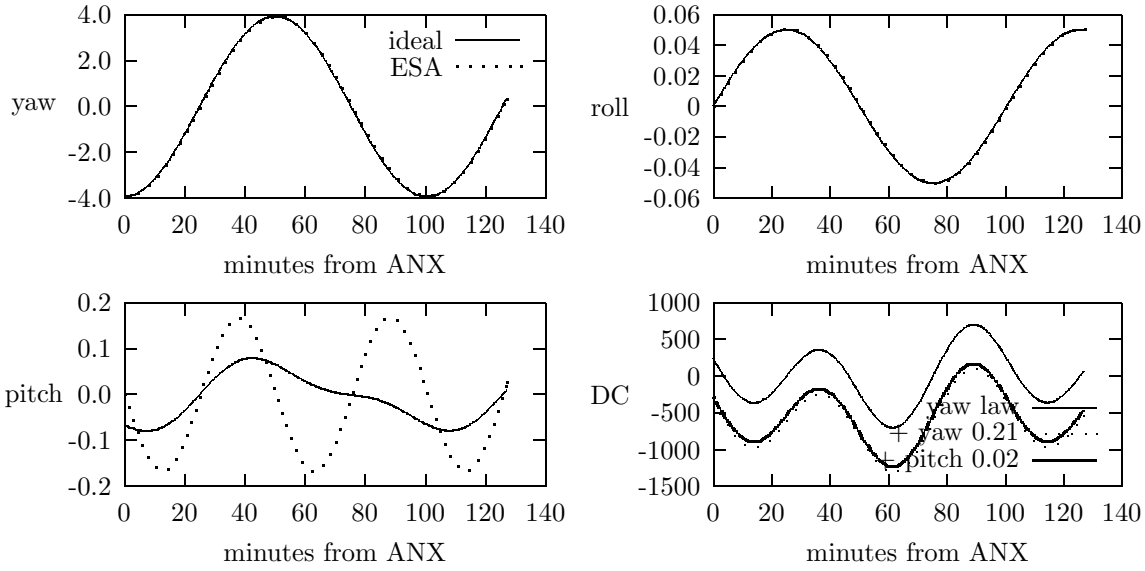

Figure 1: ASAR steering (in degrees) and expected DC for IS7 (in Hz)

ATTITUDE REFERENCE MODELS

We use the Earth center inertial (ECI) system for all calculations. Two local right-hand reference systems fixed to the satellite will also be considered. The first one is the flight reference systems adopted by CSA for RADARSAT-1 attitude measurements and defined as follows. The Z axis is pointing downwards to nadir, X is parallel to the ground-track ECI velocity, relative to the Global Ellipsoid. The Y axis is in the direction of the vector product of Z and the ECI velocity (Y points to the right). The other system is slightly offset from the flight frame. Its Z' axis points to the Earth center and Y' is in the direction of the vector product of Z' and the ECI velocity. This reference frame is very closely aligned with the actual physical body of a freely orbiting satellite which has an adequate rotation rate and zero attitude. This system is equivalent to the ESA local orbital system, excepting the orientation of the two axes (up/down and left/right).

The transformation matrix $\mathbf{B}$ from the $X'Y'Z'$ to the ECI system can be expressed in terms of the ECI state vector as shown in the Appendix. $\mathbf{B}$ depends only on the platform position (r_x, r_y, r_z) and ECI velocity (v_x, v_y, v_z). The transformation matrix $\mathbf{F}$ from XYZ system to ECI system can be expressed similarly in terms of the state vector position and velocity (in ECI) and one additional parameter (Δ_z), namely the location of the intercept between the Global Ellipsoid rotation axis and the geodetic vertical (easily calculated from the geodetic parameters).

At the level of first order approximation in steering angles yaw ϕ_y and pitch ϕ_p, the ideal zero-Doppler steering with respect to the XYZ reference system is:

$$\tilde{\phi}_y = -\frac{v_r}{v_a} \tag{4}$$

$$\tilde{\phi}_p = \frac{v_u}{v_a} \tag{5}$$

where v_u, v_r and v_a are the upward, right and ahead projections of the relative velocity [7], which takes into account Earth rotation (see Appendix). The actual ASAR beam steering law, expressed in XYZ system is:

$$\phi_y = \tilde{\phi}_y \tag{6}$$

$$\phi_p = 0 \tag{7}$$

$$\phi_r = 0 \tag{8}$$

with yaw about $+Z$, pitch about $+Y$ and roll about $+X$. The ideal zero-Doppler steering and the actual steering law, expressed in the $X'Y'Z'$ system (via transformation by $\mathbf{B}^{-1}\mathbf{F}$) are plotted in Fig. 1 for one ENVISAT orbit. They are in complete agreement with the ESA provided equations for the steering law (except for the

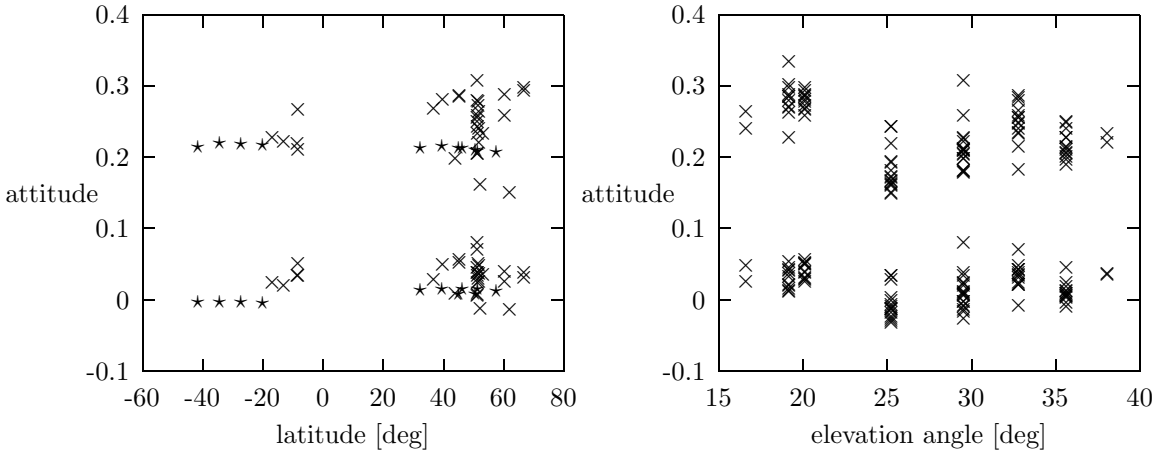

Figure 2: ASAR yaw (upper) and pitch (lower) estimates in $X_AY_AZ_A$ ("×" single beam, "⋆" WS)

sign of yaw, due to a different convention). ESA equations are given as a function of the satellite true argument of latitude, ours in terms of the state vectors. We can define the new system $X_AY_AZ_A$ centered at the satellite and rotated from XYZ by the steering angles $(\phi_y\phi_p\phi_r)$ as chosen by ESA. We have adopted $X_AY_AZ_A$ as the reference system for estimating ASAR attitude and we have included (4) in the term $f_m(\gamma)$ in (1).

All analyzed ASAR data show an offset in yaw and a minor offset in pitch relative to $X_AY_AZ_A$. Many examples have lead us to introduce an additional term in $f_m(\gamma)$ to take into account this effect. Setting the yaw offset in the physical model $\bar{\phi}_y = 0.21$ degrees and the pitch offset $\bar{\phi}_p = 0.02$ degrees (in agreement with [9]), DC can be predicted very well for any beam in every processing block. The IS7 example is shown in Fig. 1. In GASP we set the yaw offset in the physical model to be $\bar{\phi}_y = 0.23$ degrees and neglected the small pitch offset, $\bar{\phi}_p \approx 0$. The exact value of the offset is not critical as long as it is in the ballpark. The current GASP values for the offset, though not quite precise, provide DC prediction to well within one PRF. If larger discrepancies are detected in future, the GASP offset values will be reconfigured.

Since RADARSAT-1 is not steered, we could adopt either the XYZ or the $X'Y'Z'$ system as reference $(\phi_y = \phi_p = \phi_r)$. We will use the XYZ system, because it is consistent with the CSA convention. This leaves unmodeled small pitch values, which vary around the globe. Many examples confirm this effect.

RADARSAT-1 pointing includes an additional systematic squint which is elevation dependent. For elevation angles between 15 and 40 degrees this equivalent squint $\bar{\phi}(\gamma)$ varies about 0.5 degrees. It must be taken into account when estimating attitude from Doppler measurements. It is also included in $f_m(\gamma)$ in (1). The existing squint model is inaccurate for the extended beams, but it is sufficiently precise for the standard (S), fine (F) and wide(W) beams. Precise Doppler estimation on many SCW scenes led in the past to a slight modification of the CSA model [6] [8]. When the beam offset effect is properly modeled, RADARSAT-1 shows amazingly small, beam independent, residual attitude. No trends or large squints have been observed. Therefore we set no bias $(\bar{\phi}_y = \bar{\phi}_p = \bar{\phi}_r)$. Some irregular rapid attitude variations have been observed.

EXAMPLES OF ATTITUDE ESTIMATES

In GASP the attitude reference model is configurable and adjustable to suit the particular mission. The reference system for estimating the residual attitude is also configurable. We use $X_AY_AZ_A$ for ASAR, XYZ for RADARSAT-1.

Fig. 2 shows the estimated ASAR attitude (in $X_AY_AZ_A$ system) from 15 AP, 16 IM and 11 WS cases from various geographic regions. As expected, the estimates originating from WS data are much more consistent. The estimates made on single beams include the AP and IM data, as well as the single beam estimates extracted from WS data for the purpose of this analysis. Clearly, the estimation error has a larger variance for all single beam cases. Additionally, the second plot indicates a dependence of both yaw and pitch estimates on elevation angle. Yaw and pitch variations over the elevation angle appear to be correlated.

Attitude tracking examples are shown in Fig. 3. The plots show yaw and pitch tracking for a long IS4

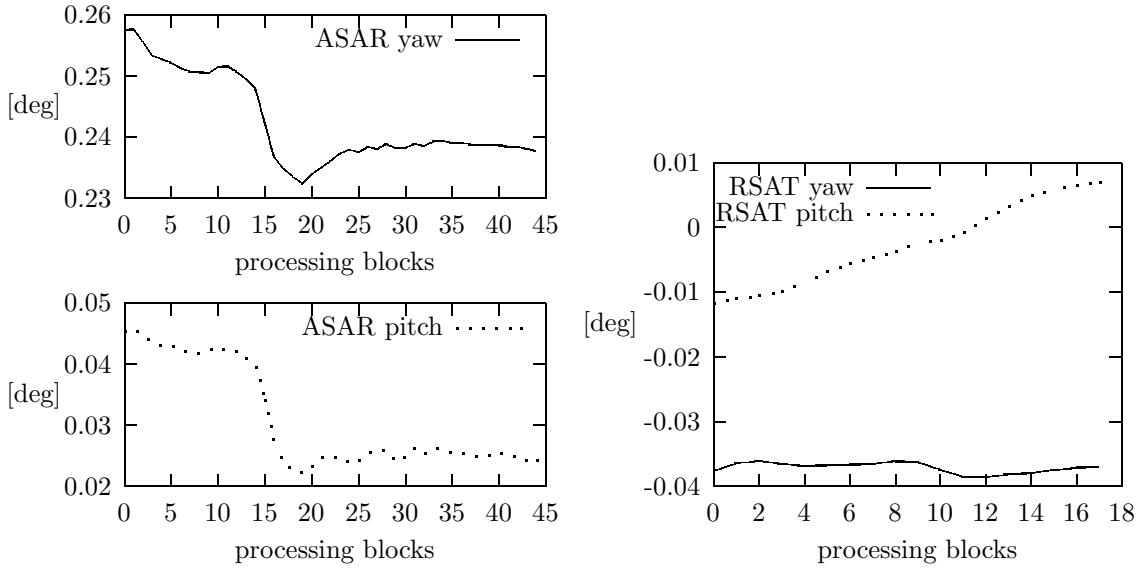

Figure 3: Attitude tracking (in $X_A Y_A Z_A$ for ASAR, in XYZ for RADARSAT-1)

(HH) data take (about 100s). The first part is over the Atlantic ocean and the second part is over Flevoland. The difference in the estimated attitude corresponds to a difference in the DC of about 20 Hz between sea and land estimates.

An example of attitude estimates (in XYZ system) for a recent (orbit 39992) RADARSAT-1 SNA pass is also shown. Yaw is steady and pitch is more variable, as is often the case.

Estimation precision depends on the beam (swath) and mode for both systems, but, generally, it is high. Different DC refinement methods produce consistent estimation results. For ASAR there is a slight disagreement between the AP components and, as illustrated, between the WS components.

WAVELENGTH DIVERSITY AND INCONSISTENCY

A combination of (2) and (3) can be used to estimate the ambiguity number. The difference between the DC estimates from two different range looks is relatively very noisy and the factor f_0/f_Δ in (2) is very large. Much averaging is needed to obtain statistically stable estimates. Generally, the technique works for RADARSAT-1. It works better for larger bandwidth (F) beams. For ASAR the same algorithm seems to converge to wrong values. Furthermore, these values depend on f_Δ. The introduction of a "system offset frequency" [9] may or may not be an elegant way out. Such offset frequency is not needed for RADARSAT-1.

Two diagrams in Fig. 4 illustrate the problem. The plots show the average difference between the estimated DC and the reference (expected) value for two RADARSAT-1 and two ASAR scenes. DC is estimated for 10 different range looks. The reference value is computed for the central wavelength and used for all looks. Upon averaging across and along swath, the slope of the plots should reveal the full DC. This can be verified for the two RADARSAT-1 scenes, one from an ascending S1 pass (negative DC), the other from a descending S7 pass (positive DC). No similar conclusion can be made for the two ASAR scenes. One of the datasets, IS4 in the descending pass, has a DC very close to 0, while the other one, IS6 in ascending pass, actually has the ambiguity number -1. This is not evident from the plots. The two datasets have different polarization, but a similar nonlinear property.

MULTI-BEAM AND WIDE SWATH INCONSISTENCY

PRF ambiguity in beam overlap [2] can be exploited for DC ambiguity resolution for RADARSAT-1 SCN and SCW modes and for ASAR WS mode. For both systems it is necessary to limit the search for the optimal ambiguity numbers to reasonable values. We set the range of possible ambiguity numbers to ± 12 for RADARSAT-1

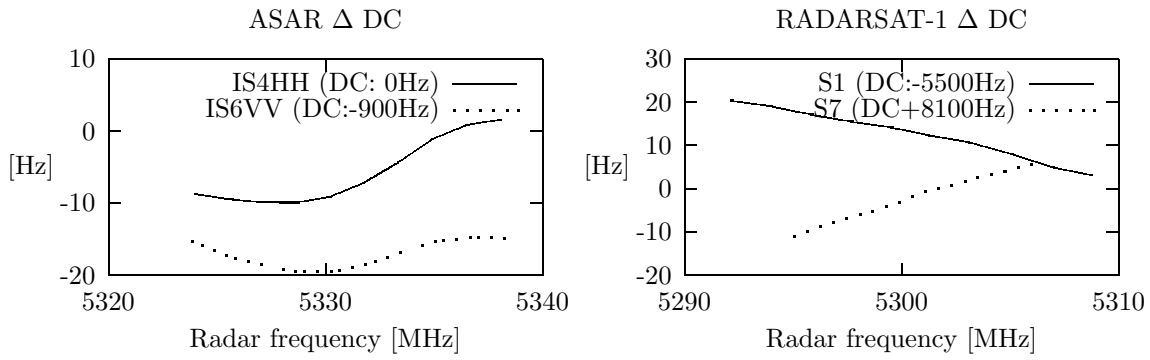

Figure 4: RADARSAT-1 and ASAR DC estimates vs. range look central frequency

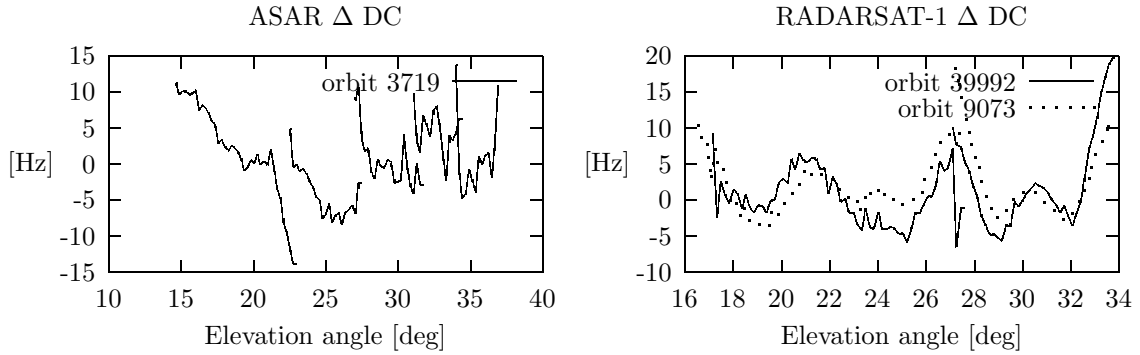

Figure 5: RADARSAT-1 and ASAR estimated DC inconsistency for multiple beams

and to ±2 for ASAR. Due to a larger DC (pointing) "gap" between ASAR beams a wider range might result in false values.

Besides satisfying (3) for pairs of beams in beam overlaps, the DC estimates must follow the form of change across swath which is consistent with (1). The combination of models (1) and (3) for multi-beam, wide swath modes offer the best opportunity to simultaneously estimate the attitude and the ambiguity numbers. The change of the ambiguous DC estimate across swath may itself reveal the full DC, according to (3), if the swath is wide enough. PRF diversity additionally contributes to the ambiguity resolution.

RADARSAT-1 is better behaved in this sense as illustrated by Fig. 5. Both plots represent the averaged residual difference between the refined DC estimates and the over-all fit based on the physical model. Two SNA RADARSAT-1 datasets are presented. They were acquired in an interval of 5 years (orbits 09073 and 39992). The residual ripples are similar and small. They are probably due to the squint model deficiency. The model is polynomial in elevation angle, which is probably inadequate.

The ASAR plot shows a higher level of discontinuity between beams. The over-all fit of the physical model is still successful. It could be improved by modeling the slight attitude differences between beams. Fig. 5 suggests a different possibility. The discontinuity seems to be related to a beam edge deviation. Also, a correction which depends continuously on the elevation angle may be appropriate, similar to the RADARSAT-1 case, but much smaller. The waveform of the correction wrt elevation angle resembles the shape seen in Fig. 2.

CONCLUSION

The main cause of ASAR non-zero DC is the inadequate pitch steering.

All Doppler estimation methods are very sensitive to slight variations of the azimuth beam pointing. Many factors affect the ASAR azimuth antenna beam pattern: beam type, frequency, polarization, mode. ASAR requires more complex physical modeling than RADARSAT-1. In the absence of very detailed physical models certain techniques (e.g. MLCC), which work for RADARSAT-1, fail for ASAR.

PRF diversity approach is statistically better than the wavelength diversity approach in almost all analyzed multi-beam cases, but the domain of the ambiguity search must be limited for ASAR. The method works especially well when extended to the full swath via physical modeling. The combined Doppler estimator described in [7] works very reliably for multi-beam modes of both missions.

For RADARSAT-1 and ASAR strip-map modes and ASAR AP mode the most reliable method for resolving the DC ambiguity is based on the physical model. The application of the physical model makes sense if and only if various misalignments are accounted for and regularly monitored. Prompt distribution of such monitoring results would be very beneficial for SAR processors which, like GASP, use physical modeling of DC (Doppler rate is derived thereafter).

For lengthy passes, DC must be updated. For the lengthy RADARSAT-1 passes attitude tracking is necessary on top of geometry updating due to possible attitude variations. ASAR attitude appears to be more stable even within long scenes.

Long-term and medium-term, however, RADARSAT-1 continues to be stable and predictable with no major attitude drifts. For ENVISAT it remains to be seen.

APPENDIX - BASIC EXPRESSIONS

The physical model (1), the steering model (4), (5) and the transformation matrix between XYZ and $X'Y'Z'$ can all be expressed explicitly in terms of the state vector, the Earth angular rotation velocity ω and the local geodetic parameter $\Delta_z = (R_e^2/R_p^2 - 1)(r_z - H\sin\eta)$, where R_e and R_p are the Earth semi-major and semi-minor axes, H is altitude above Ellipsoid and η geodetic latitude:

$$
\begin{aligned}
f_a &= -\frac{2}{\lambda} v_a \\
f_t(\gamma) &= -\frac{2}{\lambda}(v_u \cos\gamma + v_r \sin\gamma) \\
f_m(\gamma) &= \begin{cases} \bar{\phi}(\gamma) f_a & \text{for RADARSAT-1} \\ ((\bar{\phi}_y + \tilde{\phi}_y)\sin\gamma - \bar{\phi}_p \cos\gamma) f_a & \text{for ASAR} \end{cases} \\
v_a &= v_h(\Delta_z) - \omega \frac{r_x v_y - r_y v_x}{v_h(\Delta_z)} \\
v_u &= v_v(\Delta_z) \\
v_r &= \omega \frac{r(\Delta_z) v_z - (r_z + \Delta_z) v_v(\Delta_z)}{v_h(\Delta_z)} \\
\mathbf{F} &= \mathbf{T}(\Delta_z, r_x, r_y, r_z, v_x, v_y, v_z) \\
\mathbf{B} &= \mathbf{T}(0, r_x, r_y, r_z, v_x, v_y, v_z) \\
\mathbf{T}(\delta, r_x, r_y, r_z, v_x, v_y, v_z) &= \frac{1}{r(\delta) v_h(\delta)} \begin{bmatrix} r(\delta)v_x - r_x v_v(\delta) & (r_z+\delta)v_y - r_y v_z & -r_x v_h(\delta) \\ r(\delta)v_y - r_y v_v(\delta) & r_x v_z - (r_z+\delta)v_x & -r_y v_h(\delta) \\ r(\delta)v_z - (r_z+\delta)v_v(\delta) & r_y v_x - r_x v_y & -(r_z+\delta)v_h(\delta) \end{bmatrix} \\
r^2(\delta) &= r_x^2 + r_y^2 + (r_z + \delta)^2 \\
r(\delta) v_v(\delta) &= r_x v_x + r_y v_y + (r_z + \delta) v_z \\
v_h^2(\delta) &= v_x^2 + v_y^2 + v_z^2 - v_v^2(\delta)
\end{aligned}
$$

References

[1] S. N. Madsen, "Estimating the Doppler Centroid of SAR Data", *IEEE Trans. on AES*, vol. 25, pp. 134-140, March 1989.

[2] C.Y. Chang and C. Curlander, "Application of the Multiple PRF Technique to Resolve Doppler Centroid Estimation Ambiguity for Spaceborne SAR", *IEEE Trans. on GE*, vol. 30, pp. 941-949, Sept. 1992.

[3] F. H. Wong and I. G. Cumming, "A Combined SAR Doppler Centroid Estimation Scheme Based upon Signal Phase", *IEEE Trans. on GE*, vol. 34, pp.696-707, May 1996.

[4] M. Y. Jin, "Optimal Range and Doppler Centroid Estimation for a ScanSAR System", *IEEE Trans. on GE*, vol. 34, pp. 479-488, March 1996.

[5] K. Eldhuset, "Accurate Attitude Estimation Using ERS-1 SAR Raw Data", *Int. J. Remote Sensing*, vol. 17, no. 14, pp. 2827-2844, 1996.

[6] S. Marandi, "RADARSAT Attitude Estimates Based on Doppler Centroid Measurements", *CEOS Workshop on RADARSAT Data Quality*, Montreal, Québec, Feb. 1997.

[7] M. V. Dragošević and B. Plache, "Doppler Tracker for a Spaceborne ScanSAR System", *IEEE Trans. on AES*, vol. AES-36, July 2000.

[8] M. V. Dragošević, "On Accuracy of Attitude Estimation and Doppler Tracking", *Proc. CEOS SAR Workshop*, Toulouse, France, pp.127-130, Oct. 1999.

[9] B. Rosich, "Preliminary Doppler Analysis on ASAR Products", *Proceedings of the ENVISAT Calibration Review*, Nov. 2002.